TRANSLATIONAL CHEMISTRY
AN INTERFACE JOURNAL
HTTPS://WWW.TRANSLATIONALCHEMISTRY.COM/

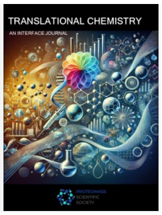

ORIGINAL ARTICLE | DOI: 10.5584/translationalchemistry.v1i1.241

Enhancing Luminescent Solar Concentrators with Aggregation-Induced Emission Fluorophores: Overcoming ACQ for Efficient Light Harvesting in PMMA Films

Antonino Oliveri[1], Alberto Picchi[1], Qiuli Zhao[2], Jing Zhi Sun[2], Marco Carlotti[1,*], Andrea Pucci[1,3], Ben Zhong Tang[4], Tarita Biver[1,3,*]

[1] Dipartimento di Chimica e Chimica Industriale, Università di Pisa, Via Moruzzi 13, 56124 Pisa, Italy. [2] Department of Polymer Science and Engineering, Zhejiang University, Hangzhou 310027, China. [3] INSTM, UdR Pisa, Via Moruzzi 13, 56124 Pisa, Italy. [4] School of Science and Engineering, The Chinese University of Hong Kong, Shenzhen (CUHK-Shenzhen), Guangdong 518172, China

Received: March 2025 **Accepted:** April 2025 **Available Online**: June 2025

Abstract

The development of efficient and stable luminescent solar concentrators (LSCs) requires fluorophores with high photoluminescence quantum yield (QY), minimal self-absorption, and robust solid-state performance. In this work, we investigate the optical properties and device performance of a red-emitting, aggregation-induced emission (AIE)-active fluorophore, [N,N'-dicyclohexyl-1,7-bis(4'-(1',2',2'-triphenyl)vinyl) phenylperylene-3,4:9,10-tetracarboxylic bisimide] (1,7-DTPEPBI), embedded in poly(methyl methacrylate) (PMMA) thin films. The dye was characterized in solution and polymer matrices, revealing excellent absorption characteristics and AIE behavior in solvent/non-solvent mixtures. In PMMA films, 1,7-DTPEPBI displayed concentration-dependent fluorescence, with a maximum QY of 37% at 0.4 weight % and a red-shifted emission ideal for LSC applications. LSC devices were fabricated using solution-cast PMMA films doped with the dye at varying concentrations. Optical characterization showed an internal photon efficiency (η_{hint}) up to 29% and minimal self-absorption losses, confirmed by P_0 values close to 0.9. Despite lower external photon efficiency (η_{ext}) and device efficiency (η_{dev}) compared to benchmark fluorophores, the AIE-active 1,7-DTPEPBI demonstrated potential as a solid-state emitter for thin-film LSCs, especially in configurations requiring reduced dye reabsorption and good long-term photostability.

Keywords: Luminescent solar concentrators, aggregation-induced emission, poly(methyl methacrylate), optical efficiencies, device efficiency.

Introduction

The global transition toward renewable energy sources has driven extensive research into solar energy harvesting technologies. Among these, luminescent solar concentrators (LSCs) have gained significant attention as cost-effective alternatives to traditional photovoltaic (PV) panels [1,2]. LSCs consist of transparent waveguiding slabs embedded with high-quantum-yield fluorophores that absorb sunlight and re-emit it at longer wavelengths [3]. Through total internal reflection (TIR), the emitted photons are guided toward the edges of the slab, where photovoltaic cells convert them into electricity. Compared to conventional PV modules, LSCs offer lightweight, scalable, and versatile solutions that integrate well with building-integrated photovoltaics (BIPV), enabling applications in windows, facades, and urban energy harvesting systems [4,5]. A crucial component of LSC efficiency is the selection of high-performance fluorophores capable of absorbing a broad portion of the solar spectrum while exhibiting high fluorescence quantum yield (QY), minimal self-absorption, and long-term photostability [6]. Traditional organic fluorophores such as perylene derivatives, rhodamines, and coumarins have been widely used due to their strong absorption, tunable emission, and high solubility in polymer matrices [7]. However, a major limitation of many organic fluorophores is aggregation-caused quenching (ACQ) – a phenomenon where molecular aggregation leads to non-radiative relaxation, drastically reducing fluorescence efficiency in solid-state applications [8]. This effect is particularly detrimental for LSCs, where high dye loading is often required to maximize light absorption. To address this challenge, fluorophores exhibiting aggregation-induced emission

***Corresponding author:** Dr. Marco Carlotti, Email: marco.carlotti@unipi.it | Prof. Tarita Biver, E-mail: tarita.biver@unipi.it

(AIE) have emerged as promising candidates for next-generation LSCs [9]. Unlike conventional fluorophores that experience ACQ, AIE-active materials are non-emissive in dilute solutions but exhibit strong fluorescence upon aggregation due to the restriction of intramolecular motions (RIM) [10,11]. This mechanism effectively suppresses non-radiative decay channels, enabling bright emission in the solid state. Among the most studied AIE-active compounds are tetraphenylethylene (TPE) derivatives, which have demonstrated enhanced stability, minimal self-absorption, and excellent processability in polymer matrices [12–16].

Recent studies have demonstrated the successful incorporation of AIE luminogens into poly(methyl methacrylate) (PMMA) films for LSC applications [17–20]. PMMA remains the benchmark polymer matrix for LSCs due to its high optical transparency, chemical resistance, and compatibility with a wide range of fluorophores [21]. In particular, TPE-based fluorophores have been widely investigated for their ability to maintain high fluorescence efficiency under concentrated conditions, effectively mitigating aggregation-caused quenching (ACQ). Among them, several donor –acceptor TPE derivatives, such as TPE-MRh [22] and TPE-BPAN [23] have demonstrated aggregation-induced emission (AIE) behavior, red-shifted emission, and promising quantum yields when embedded in polymer matrices. These red-emitting TPE systems have shown excellent compatibility with PMMA and have enabled long-term photostability and efficient light harvesting in both thin-film and bulk LSC architectures. Such characteristics make them ideal candidates for enhancing the performance and durability of next-generation luminescent solar concentrators

In this study, the fluorophore [N,N’-dicyclohexyl-1,7-bis(4’-(1’,2’,2’-triphenyl)vinyl)phenylperylene-3,4:9,10-tetracarboxylic bisimide] (1,7-DTPEPBI) (**Figure 1A**) [24], was selected for its dual structural advantage: it merges the strong light-harvesting and red-emitting properties of perylene bisimides (PBIs) with the AIE behavior of the TPE units. The specific substitution at the bay position of the perylene core with TPE moieties is designed to suppress the detrimental π–π stacking interactions typical of PBIs, which are known to cause fluorescence quenching in the solid state. At the same time, the presence of TPE enables AIE, ensuring that fluorescence is activated upon aggregation, as occurs in polymer matrices and thin films. This tailored molecular design was conceived to retain high photoluminescence efficiency under the concentrated and condensed conditions typical of LSCs, while minimizing reabsorption losses and enhancing photostability. Compared to other TPE-based AIEgens, 1,7-DTPEPBI also offers extended spectral coverage in the red region and improved compatibility with PMMA, making it a particularly suitable candidate for solid-state light-harvesting applications (**Figure 1B**) [25,26]. This study investigates the optical and photovoltaic performance of this AIE-active red-emitting fluorophore in PMMA -based LSCs. LSCs are evaluated for their light-harvesting capabilities, fluorescence quantum yield, and resistance to photodegradation under prolonged solar exposure with the aim to demonstrate the feasibility of AIE-based materials in enhancing the sustainability and efficiency of LSC technology.

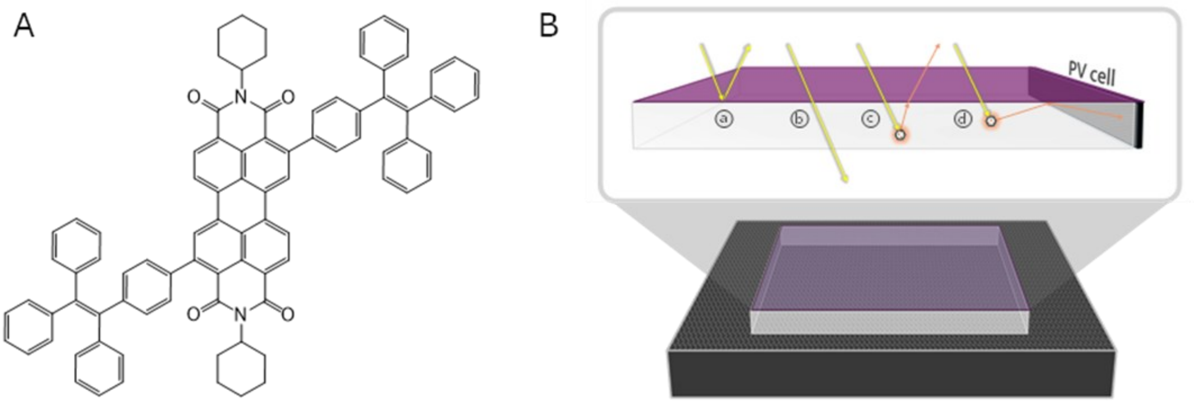

Figure 1 | (A) Molecular structure of [N,N’-dicyclohexyl-1,7-bis(4’-(1’,2’,2’-triphenyl)vinyl)phenylperylene-3,4:9,1’-tetracarboxylic bisimide] (1,7-DTPEPBI); (B) Interactions of photons within an LSC. In particular: a) reflection; b) transmission; c) photon losses by outward refraction; d) emitted photon reaching the PV cell on the LSC edge.

Material and Methods

Materials

The [N,N’-dicyclohexyl-1,7-bis(4’-(1’,2’,2’-triphenyl)vinyl) phenylperylene-3,4:9,1’-tetracarboxylic bisimide] (1,7-DTPEPBI, **Figure 1A**) was synthesized in a previous work [24]. The molar concentration of the dye will be indicated as CD. Poly(methyl methacrylate) (PMMA) was from Merck, average Mw ~350,000 by GPC, density 1.17 g/mL at 15.0 °C.

All solvents used in present work were the ultrapure reagent: acetone (ACS reagent, > 99.5%, Merck); acetonitrile (HPLC-GOLD -Ultragradient Grade, Carlo Erba); chloroform (Spectrophotometric Grade, > 99.5%, Alfa Aesar); hydrochloric acid (ACS reagent, 37%, Merck); diethylether (ACS reagent, ≥99.8%, Merck); dimethysulphoxide (≥99.9%, Merck); ethanol (≥99.8%, Merck); hexane (for HPLC, ≥97.0%, Merck); methanol (Spectrophotometric Grade, 99.8+%, Alfa Aesar); tetrahydrofuran (ACS reagent, > 99.9%, Honeywell or Spectrophotometric Grade, 99.7+%, Alfa Aesar); toluene (Spectrophotometric Grade, 99.7+%, Alfa Aesar).

Methods

Preliminary solubilization tests (0.5 mg in 1.5 mL solvent) showed that 1,7-DTPEPBI is insoluble in acetone, acetonitrile, diethyl ether, dimethysulphoxide, hexane and methanol. It is, instead, soluble in chloroform, tetrahydrofuran (THF) and toluene which were thus chosen for the characterization in solution of the dye. Stock solutions of the dye in each of the solvents were done by weight. In brief, 2-3 mg of 1,7-DTPEPBI (MW = 1251.5 g/mol) were added to 1.0 mL of solvent (chloroform, THF or toluene). These mother solutions (ca. 2 mM) were diluted either with the same solvent or with the appropriate solvent/non-solvent mixtures (v/v%) to obtain working solutions for both UV-vis and fluorescence experiments. For the solution spectra, UV-vis data were collected using a Perkin-Elmer Lambda 650 spectrophotometer. Absorption spectra were recorded in the wavelength range from 200 nm to 800 nm, usnig slit width 2 nm, spectral resolution 1 nm, integration time 0.2 s; quartz cuvettes of the "macro" type (minimum volume 1000 μL), with an optical path of 1.0 cm, were used. In the experiments at different concentrations, increasing amounts of the working solutions were added directly in the spectrophotometric cuvette by means of a Hamilton micro-syringe connected to a Mitutoyo micrometric screw (1 turn = 8.2 μL). An Agilent Technologies Cary 5000 Series UV-Vis-NIR spectrophotometer was used for the spectrophotometric characterization of the polymeric matrices. The polymer films were housed in a solid sample holder and three absorption spectra were recorded, one at the center and two at the edges.

Spectrofluorimetric measurements were done on a Perkin Elmer LS55 instrument, using semi-micro cuvettes (minimum volume 500 μL) with an optical path of 1.0 cm. Fluorescence spectra were recorded by exciting at different absorption maxima and emission wavelength range typically from λ_{ex} to 800 nm, using slit widths both 3 nm, spectral resolution of 1 nm, integration time of 0.5 s. In the experiments at different concentrations, increasing amounts of the working solutions were added directly in the spectrofluorimetric cuvette by means of the already cited Hamilton micro-syringe. In the case of the polymeric films, the fluorescence tests used a Horiba Jobin Yvon FluoroLogR-3 instrument. The polymer films were analyzed using the solid sample holder and placing the detector in front-face mode (30°, FF) to avoid the interference of scattered light. The quantum yield measurements performed on the solid-state samples were obtained using a 152 mm diameter Quanta-phi integrating sphere, coated in Spectralon® and positioned on the optical path of the Horiba Jobin Yvon FluoroLogR-3 spectrofluorometer.

The LSC was fabricated on a high-purity optical glass substrate measuring 50.0 × 50.0 × 3.3 mm, specifically an Edmund Optics BOROFLOAT® window (50 × 50 mm, TS grade). This glass is maintained in 6 N HCl for one night, then rinsed with water, acetone and ethanol. To prepare the solution to be cast, 60.0 mg of polymer were mixed with a known quantity of chloroform solution containing the fluorophore to obtain a mixture at a known weight % in the 0.2-2.0% range. The mixture is made up to 1.5 mL volume and shaken to ensure solubilization. This latter mixture is thus dropped on the glass following a solution casting procedure. The films were left to dry for 24 h, then detached from the glass support by immersion in Ultra-Pure water. The film thickness was controlled by Rupac-Digitronic micrometer with 0-25 mm measuring range, 0.001 mm resolution and ± 4 μm precision. The surface of the polymer films, still adhered to the preparation glass, was investigated by an LED epifluorescence microscope from AUXILAB S.L., code HBF002, connected to a 2.3 Mega Pixel Invenio 2EIII camera and a personal computer equipped with the DeltaPix InSight software. The images were acquired working both in transmission and epifluorescence.

Results and discussion

Solution studies

To thoroughly investigate the optical properties of 1,7-DTPEPBI in solution, we performed UV-Vis absorption and fluorescence measurements in three selected solvents (chloroform, THF, and toluene) and in different solvent/non-solvent systems in which the dye was dispersed. **Figure 2** shows the absorbance profiles of 1,7-DTPEPBI in the different solvents. In agreement with the literature, there are four maxima: the two at shorter wavelengths are related to the tetraphenylethylene groups [27,28], while those at lower energies are due to the perylene core [29]. UV-Vis absorption spectra were recorded for different dye concentrations (CD), approximately in the 2×10^{-6} M to 1×10^{-4} M range (**Figure S1**).

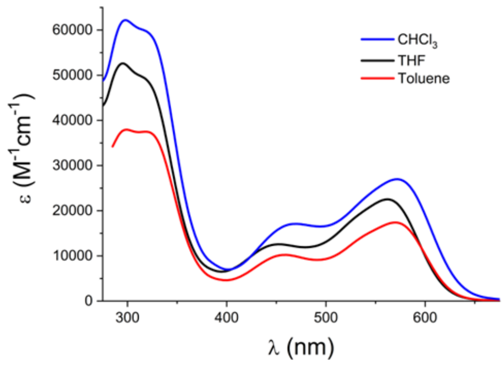

Figure 2 | Absorbance profiles of 1,7-DTPEPBI in different solvents, 25.0 °C.

The shapes do not seem to change with increasing concentrations, as it would have occurred in the presence of auto-association processes.

The absorbance vs. concentration test is done to further inspect any possible aggregation phenomena. Data are analyzed both for linearity (Lambert-Beer plots) (**Figure S2**) and using the absorbance ratio at two different wavelengths (**Figure S3**). The latter approach emphasizes also subtle deviations from direct proportionality. None of the experiments done evidenced auto-aggregation effects under the conditions of the experiments. The photophysical parameters are collected in **Table 1**.

We thus checked the possible light emission characteristics of 1,7-DTPEPBI in the three selected solvents, at a concentration of ca. 1×10^{-6} M and excitation at each of the absorbance maxima. Given that 1,7-DTPEPBI was designed to show AIE characteristics, an absence of fluorescence emission is expected in a good solvent [10]. This was indeed the case for chloroform and THF. On the other hand, the measurements in toluene revealed a signal centered at $\lambda_{MAX,em}$ = 630 for $\lambda_{MAX,ex}$ = 570 nm (**Figure S4**), indicating that the dye molecules are at least partially in the form of an aggregate in hydrophobic solvents [24]. The light emission is proportional to concentration and the limit of detection of 1,7-DTPEPBI in toluene (LOD = 3σ of the blank) is found to be 2.40×10^{-8} M (**Figure S5**).

The AIE characteristics of 1,7-DTPEPBI were then inspected by dispersing it in different solvent/non-solvent systems. In particular, we considered THF/H_2O, $CHCl_3$/Hexane, $CHCl_3$/Methanol and Toluene/Hexane mixtures. The absorption and fluorescence properties of each system were analyzed as the percentage of non-solvent increased, keeping the dye concentration constant. In agreement with AIE, light emission switches on as the non-solvent content increases. For THF/H_2O (**Figure S6**), AIE light-on is detectable already at 10% H_2O but significant precipitation occurs for $H_2O\% \geq 40\%$. Note that the precipitates are amorphous (the solid does not emit any light) [30]. For $CHCl_3$/Hexane mixtures (**Figure S7**) the low polarity of both solvents suppressed precipitation phenomena and enabled to test all the possible compositions of the mixtures; **Figure 3A** shows the AIE effect for this system. In this more favorable case, we also collected an EEM plot (**Figure S8**). Switching to $CHCl_3$/Methanol produced dye precipitation at 70% Methanol and a reduced light switch effect (**Figure S9**). Finally, in Toluene/Hexane mixtures, 1,7-DTPEPBI started to precipitate at 70% Hexane; as already cited, an emission signal is present also at 0% Hexane, but it further increases with the non-solvent content (**Figure S10**). **Figure 3B** collects the variation of the fluorescence signals as a function of the percentage of non-solvent present in solution, comparing the behavior of the different solvent/non-solvent systems. It is interesting to note that the emission band of the highly emissive aggregates formed in $CHCl_3$/Hexane and Toluene/Hexane (550-750 nm) corresponds to the optimal region for LSC applications (500-850 nm, i.e. the region of maximum photovoltaic efficiency) with a Stokes' shift of ca. 60-65 nm. Differently, THF/H_2O and $CHCl_3$/Methanol mixtures induce the formation of low emitting species with a signal centered at ca. 520 nm. Overall, $CHCl_3$ seems the solvent with the better performance.

Table 1 | UV-vis characterization of 1,7-DTPEPBI in different solvents, 25.0 °C. ε_r = polarity index; ε = molar absorption coefficient (error < 1%).

Solvent	ε_r	$\lambda_{MAX,Abs}$ (nm), ε (10^4 M^{-1} cm^{-1})			
THF	7.5	295, 5.54	323, 5.05	453, 1.27	562, 2.26
$CHCl_3$	4.8	298, 6.30	321, 6.01	470, 1.99	572, 2.83
Toluene	2.4	299, 3.99	323, 2.95	458, 1.11	570, 1.89

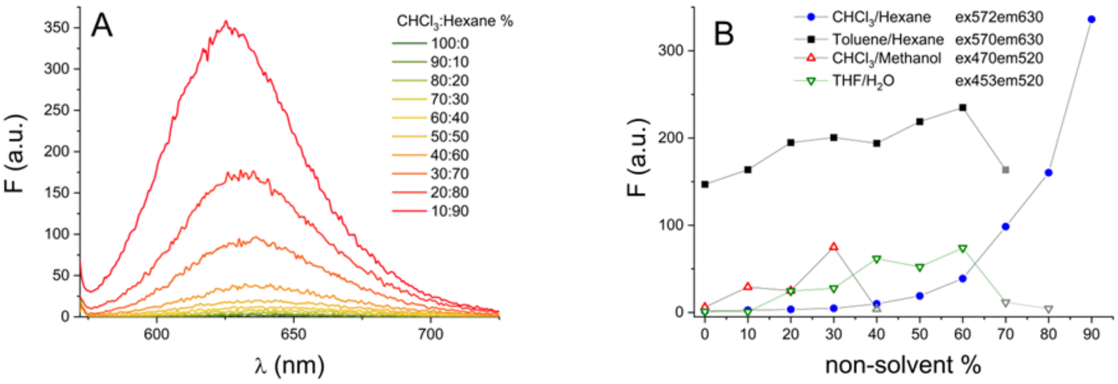

Figure 3 | (A) Fluorescence emission of 1,7-DTPEPBI in different $CHCl_3$/Hexane mixtures; $C_D = 1.66\times10^{-5}$ M, λ_{ex} = 572 nm, 25.0 °C. (B) Comparison of fluorescence light on effects at 25.0 °C for the different mixtures considered in this work (normalized at the same 1,7-DTPEPBI content; grey points are those where precipitation occurs).

2. Optical studies in polymeric films

After studying the spectroscopic properties of 1,7-DTPEPBI in solution, we investigated its behavior in polymeric films to evaluate its possible application as fluorescent dopant in luminescent devices. In particular, we employed films of poly(methyl methacrylate) (PMMA) because of its very high clarity and good processability, which makes it an ideal material for the fabrication of optical devices and clear structural components [31].

We prepared several films (thickness of 25 ± 5 μm) containing different amounts of dye, from 0.2 weight % (wt.%) to 2 wt.%, via solution casting (**Figure 4A**). The films appeared clear, with a purple coloration, and emitted red fluorescence upon exposure under UV light (366 nm; **Figure 4B**).

The absorption properties of 1,7-DTPEPBI in PMMA films closely resembled that of the dye in solution, with the most red-shifted featuring a λ_{MAX} of 564 nm and a shoulder centered at about 465 nm; conversely, we found that the fluorescence of the dye in the film was significantly different from the examples reported above in solution (**Figure 5A**). To start, the emission maximum in PMMA was red-shifted, resulting in larger Stokes shifts in this system. These latter ranged from about 99 nm, with respect to the absorption peak at 564 nm, in the case of the film with the lowest dye concentration (0.2 wt.%) and increased up to 135 nm in the case of the one with the highest (2 wt.%). The reason behind this variation in the Stokes shift with concentration is not only due to inner filter effects but also to a change in the shape of the emission profile. At low 1,7-DTPEPBI concentrations, the emission peak is symmetric and centered at about 660 nm, similar in shape to those observed in solution. This suggests that, even at the lowest concentration tested, the dye either forms emissive aggregates in the chosen PMMA matrix or that its motion is sufficiently restricted to have a significant emission. Upon investigation via fluorescence microscopy, it is possible to observe the presence of irregular aggregates of different dimensions (20-150 μm of diameter) randomly distributed within the matrix, which emitted red radiation (**Figure 4C**) throughout the concentration range tested. Nevertheless, no evidence of fluorophore segregation at the surface was observed.

As the quantity of 1,7-DTPEPBI in the film increased, a new peak appeared centered at about 700 nm. The AIE behavior of the investigated dye was noticeable even in the polymer matrix, with the maximum emission intensity increasing dramatically going from 0.2 wt.% to 0.8-1.0 wt.%. At higher concentrations, the intensity decreased again, most likely due to self-absorption phenomena and to the formation of amorphous aggregates. In these latter, fluorescence is inherently lower due to the less dense packing, which increases the intermolecular distance, making the side chains more mobile and more likely to dissipate energy through vibrational and rotational motions.

Figure 5B reports the photoluminescence quantum yield (QY) of 1,7-DTPEPBI in PMMA for the different concentrations. In particular, it was found to decrease constantly from 37 ± 4 % in the case of the less concentrated film to 10 ± 1% for the 2.0 wt.% one, suggesting the formation of amorphous, poorly luminescent aggregates, as indicated by fluorescence microscopy images. This could be related to the fact that perylene bisimides still experience progressive quenching of their emissions in PMMA, likely due to self-aggregation and energy transfer processes, notwithstanding the presence of TPE moieties at the bay positions. On the other hand, Lumogen Red in PMMA films exhibits remarkable QY stability across the entire concentration range investigated, confirming its superior resistance to aggregation-induced quenching effects [32].

The QY values for 1,7-DTPEPBI were found to be considerably lower than those of highly performing ACQ fluorophores, such as Lumogen F Red 305 (LR305) [33], benzobisthiazoles [34], benzodithiophenes [35], and quinoxalines [36,37], prepared and measured in similar conditions. However, the measured QY at a 1,7-DTPEPBI concentration of 0.4 wt.%, i.e. 37 ± 4%, is higher or comparable to that of similar AIE or AIEE systems already investigated in LSC applications [22,23,38].

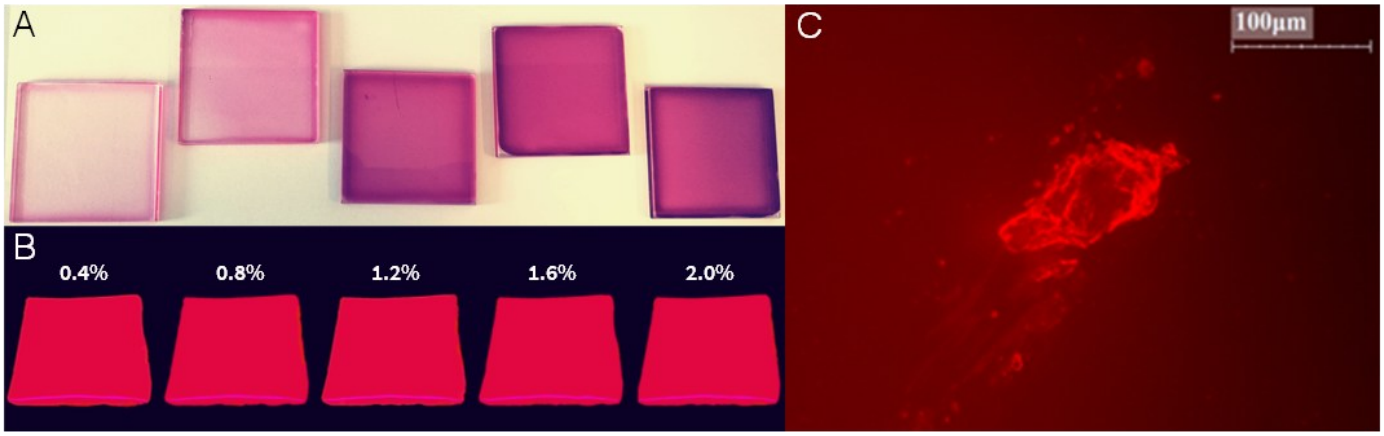

Figure 4 | Films (5×5 cm) of 1,7-DTPEPBI dispersed in PMMA; (A) under natural light; (B) under 366 nm illumination. (C) Epifluorescence microscopy image of 1,7-DTPEPBI/PMMA thin films at 0.4 wt.%.

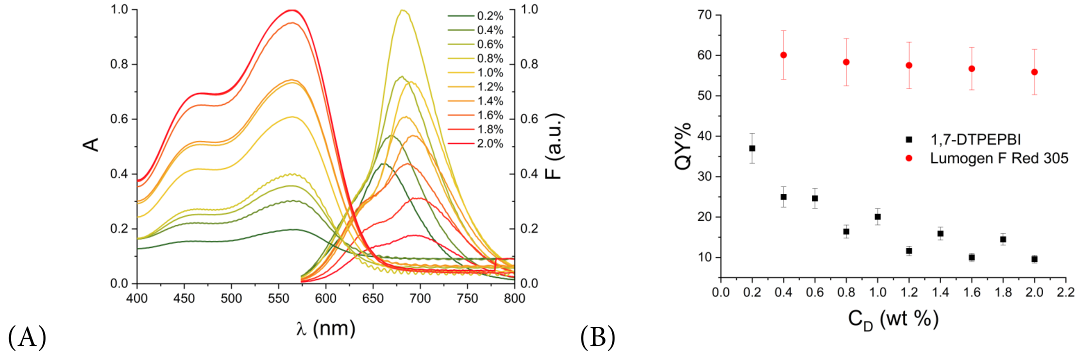

Figure 5 (A) Absorbance and fluorescence emission profiles of 1,7-DTPEPBI in PMMA; 0.2% ≤ C_D ≤ 2.0 wt.%; λ_{ex} = 564 nm. (B) Quantum yield percent (QY%) for 1,7-DTPEPBI in PMMA (λ_{ex} = 564 nm); data for the same films with Lumogen F Red 305 (λ_{ex} = 575 nm) are also shown for comparison.

Luminescent solar concentrators (LSCs) based on 1,7-DTPEPBI

Despite the non-optimal QY of the dye, we conducted further tests on PMMA films doped with 1,7-DTPEPBI to evaluate its performance as emitter in thin-film LSCs compared to previously investigated AIEgens [23,38–42]. These tests help determine whether aggregation-induced emission (AIE) effects can be effectively exploited in solid-state PMMA matrices, despite the quenching observed at higher dye concentrations. To do so, we prepared via solution casting a series of 5x5x0.4 cm LSC devices comprising thin PMMA films at different dye concentrations (0.5-2.0 wt.%) and evaluated their performances in terms of internal photon efficiency (η_{int}), representing the fraction of absorbed photons which is emitted from the edges of the device, external photon efficiency (η_{ext}), the fraction of incident photons which is emitted from the edges, and, finally, device efficiency (η_{dev}), the ratio between the incident power and the power originating from a PV module coupled to the edge of the LSC. As shown in **Figure 6A**, the internal photon efficiency, η_{int}, decreases with increasing concentration, from a value of 29 ± 2% at 0.4 wt.% to 12 ± 2% at 2.0 wt.%. This result is consistent with QY and with the formation of low-emission aggregates. Although a small concentration range of AIE occurrence, which was previously shown from 0.4 to 0.8% wt., the highest QY is observed at 0.4 wt.%. This may indicate a simultaneous formation of highly emitting aggregates, due to the AIE effect, and non-emitting amorphous aggregates, caused by ACQ. However, the decline in hint is less substantial with increasing concentration compared to QY, indicating a minimal occurrence of self-absorption, a phenomenon that is generally detrimental to the efficiency at extended photon optical paths. An estimation of self-absorption losses was provided by Wilson *et al.* [43]. Following the detailed procedure and considering as reabsorption-free an edge-emission spectrum acquired when exciting at a point close to the edge, we calculated P_0, i.e. the probability of photons nonsuffering self-absorption. As shown in **Table S1**, P_0 is approximately constant at ≈ 0.9 across the concentration range examined. This suggests that self-absorption has a limited impact, even at high fluorophore loadings. This outcome can be attributed to the thin-film configuration, which, although necessitates higher concentrations (by approximately 100 times), has a reduced volume of doped polymer, while the light-guiding effect is predominantly exerted by the glass substrate. Consequently, for most of the optical path, the emitted photons pass through the non-absorbing glass. The external photon efficiency, η_{ext}, increased with concentration until it reached almost constant values at around 2.2% (**Figure 6B**). These performances were found to be considerably lower than those of the benchmark fluorophores, with roughly a quarter of the efficiency of LR305, and also lower than the ≈3.4% calculated for recently investigated TPE-based emitters [23,40]. This decline can be attributed to the significant QY decrease from 0.8 wt.% onwards.

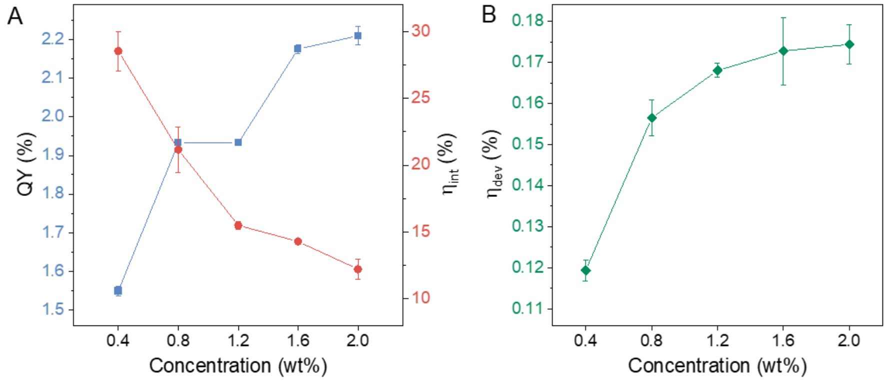

Figure 6 | (A) Quantum yield percent (QY%) and internal photon efficiency (η_{int}) for 1,7-DTPEPBI in PMMA; (B) External photon efficiency (η_{ext}) and electrical device efficiency (η_{dev}) for thin-film LSCs containing 1,7-DTPEPBI.

Concurrently, the electrical device efficiency, η_{dev}, exhibited an analogous trend to η_{ext}, increasing with concentration. η_{dev} was derived from J-V curve acquisitions without the application of a reflective tape on the edges. This approach enables the calculation of low values, which can be multiplied by 4 to simulate the scenario where solar cells are placed on all four sides [44]. Consequently, for a four-side collection configuration, $\eta_{dev,4\,sides}$ = 0.70 %. Although not directly comparable with previous literature data acquired with reflective tape on the uncovered edges, this determination is helpful to estimate the real power production of an LSC-PV system. It is important to note that only through a device scale-up reliable power production measurements can be obtained simulating real-world conditions. Nevertheless, data on photon efficiencies can be readily utilized for cross-laboratory comparisons, as outlined in the widely accepted LSC laboratory protocols [45].

Concluding remarks

This study explored the integration of a novel red-emitting fluorophore, 1,7-DTPEPBI, combining perylene bisimide and tetraphenylethylene moieties, into PMMA matrices for the fabrication of efficient luminescent solar concentrators (LSCs). Designed to exhibit aggregation-induced emission (AIE) behavior, 1,7-DTPEPBI demonstrated good solubility in selected organic solvents and excellent photostability. Spectroscopic analyses in solution confirmed the absence of aggregation-caused quenching (ACQ) and the activation of AIE properties under specific solvent/non-solvent conditions. When embedded in PMMA films, 1,7-DTPEPBI exhibited significant, red-shifted fluorescence and AIE-driven luminescence, although the quantum yield (QY) decreased at higher concentrations due to the formation of low-emissive, amorphous aggregates. Nevertheless, LSC devices fabricated with these films achieved promising optical performances. The optimal internal photon efficiency (η_{int}) was observed at 0.4 wt.% dye loading, with values progressively decreasing at higher concentrations due to partial quenching. Importantly, self-absorption losses were found to be minimal, as confirmed by high P_0 values across the concentration range. While external photon efficiency (η_{ext}) and device efficiency (η_{dev}) were lower than those achieved with benchmark fluorophores like Lumogen F Red 305, the results demonstrate the potential of AIE-based fluorophores as viable, structurally tunable alternatives for solid-state light-harvesting applications. The combination of photostability, controlled emission, and low self-absorption in thin-film configurations underscores the relevance of these systems in the ongoing development of cost-effective and scalable LSC technologies. Future work will focus on the structural optimization of AIE-active fluorophores to enhance QY at higher loadings, the exploration of new polymeric matrices with reduced aggregation tendencies, and device scaling to validate real-world photovoltaic performance.

Acknowledgements

This research is supported by PON 2014-2020 “Research and Innovation” resources – Green/Innovation Action – DM MUR 1061/2022. We also acknowledge financial support under the National Recovery and Resilience Plan (NRRP), Mission 4, Component 2, Investment 1.1, Call for tender No. 104 published on 2.2.2022 by the Italian Ministry of University and Research (MUR), funded by the European Union – NextGenerationEU – Project Title LUminescent solar Concentrators based on recycled methyl methacrylate and Eco-compatible materials (LUCE) CUP I53D23004190006 Codice progetto: 2022ZZC2HZ by the Italian Ministry of Ministry of University and Research (MUR).

References

[1] N. Aste, L.C. Tagliabue, C. Del Pero, D. Testa, R. Fusco, Renew. Energy 76 (2015) 330–337. DOI: 10.1016/j.renene.2014.11.026

[2] W.G.J.H.M. Van Sark, EPJ Web Conf. 33 (2012) 0–7. DOI: 10.1051/epjconf/20123302003

[3] S. Castelletto, A. Boretti, Nano Energy 109 (2023) 108269. DOI: 10.1016/j.nanoen.2023.108269

[4] B.S. Richards, I.A. Howard, Energy Environ. Sci. 16 (2023) 3214–3239. DOI: 10.1039/D3EE00331K

[5] F. Meinardi, F. Bruni, S. Brovelli, Nat. Rev. Mater. 2 (2017) 17072. DOI: 10.1038/natrevmats.2017.72

[6] J. Roncali, Adv. Energy Mater. 10 (2020) 2001907. DOI: 10.1002/aenm.202001907

[7] L. Beverina, A. Sanguineti, in: Sol. Cell Nanotechnol., Wiley, 2013, pp. 317–355. DOI: 10.1002/9781118845721.ch13

[8] E. Tatsi, A. Nitti, D. Pasini, G. Griffini, Nanoscale 16 (2024) 15502–15514. DOI: 10.1039/D4NR01910E

[9] J. Xu, M.H. Chua, B.Z. Tang, eds., Aggregation-Induced Emission (AIE), Elsevier, 2022. DOI: 10.1016/C2020-0-01478-7

[10] Y. Hong, J.W.Y. Lam, B.Z. Tang, Chem. Commun. (2009) 4332–4353. DOI: 10.1039/b904665h

[11] J. Luo, Z. Xie, Z. Xie, J.W.Y. Lam, L. Cheng, H. Chen, C. Qiu, H.S. Kwok, X. Zhan, Y. Liu, D. Zhu, B.Z. Tang, Chem. Commun. 18 (2001) 1740–1741. DOI: 10.1039/b105159h

[12] N. Guidugli, R. Mori, F. Bellina, B.Z. Tang, A. Pucci, in: Princ. Appl. Aggregation-Induced Emiss., Springer International Publishing, Cham, 2019, pp. 335–349. DOI: 10.1007/978-3-319-99037-8_14

[13] T.A. Geervliet, I. Gavrila, G. Iasilli, F. Picchioni, A. Pucci, Chem. - An Asian J. 14 (2019) 877–883. DOI: 10.1002/asia.201801690

[14] G. Lyu, J. Kendall, I. Meazzini, E. Preis, S. Bayseç, U. Scherf, S.

Clément, R.C. Evans, ACS Appl. Polym. Mater. 1 (2019) 3039–3047. DOI: 10.1021/acsapm.9b00718

[15] F. Yang, X. Ye, G. Chen, J. Xiao, Z. Wu, Y. Luo, W. Zheng, W. Zhou, L. Wang, B. Lu, Y. Wei, Z. Yang, Z. Chi, X. Dong, Compos. Part B Eng. 219 (2021) 108898. DOI: 10.1016/j.compositesb.2021.108898

[16] H. Wang, Q. Li, P. Alam, H. Bai, V. Bhalla, M.R. Bryce, M. Cao, C. Chen, S. Chen, X. Chen, Y. Chen, Z. Chen, D. Dang, D. Ding, S. Ding, Y. Duo, M. Gao, W. He, X. He, X. Hong, Y. Hong, J. Hu, R. Hu, X. Huang, T.D. James, X. Jiang, G. Konishi, R.T.K. Kwok, J.W.Y. Lam, C. Li, H. Li, K. Li, N. Li, W. Li, Y. Li, X. Liang, Y. Liang, B. Liu, G. Liu, X. Liu, X. Lou, X. Lou, L. Luo, P.R. Mcgonigal, Z. Mao, G. Niu, T.C. Owyong, A. Pucci, J. Qian, A. Qin, Z. Qiu, A.L. Rogach, B. Situ, K. Tanaka, Y. Tang, B. Wang, D. Wang, J. Wang, W. Wang, W. Wang, W. Wang, X. Wang, Y. Wang, S. Wu, Y. Wu, (2023). DOI: 10.1021/acsnano.3c03925

[17] J.L. Banal, B. Zhang, D.J. Jones, K.P. Ghiggino, W.W.H. Wong, Acc. Chem. Res. 50 (2017) 49–57. DOI: 10.1021/acs.accounts.6b00432

[18] J.L. Banal, K.P. Ghiggino, W.W.H. Wong, Phys. Chem. Chem. Phys. 16 (2014) 25358–25363. DOI: 10.1039/c4cp03807j

[19] W. Ma, W. Li, M. Cao, R. Liu, X. Zhao, X. Gong, Org. Electron. 73 (2019) 226–230. DOI: 10.1016/j.orgel.2019.06.017

[20] P. Meti, F. Mateen, D.Y. Hwang, Y.-E. Lee, S.-K. Hong, Y.-D. Gong, Dye. Pigment. 202 (2022) 110221. DOI: 10.1016/j.dyepig.2022.110221

[21] G. Griffini, Front. Mater. 6 (2019) 1–8. DOI: 10.3389/fmats.2019.00029

[22] C. Micheletti, Q. Wang, F. Ventura, M. Turelli, I. Ciofini, C. Adamo, A. Pucci, Aggregate 3 (2022) 1–10. DOI: 10.1002/agt2.188

[23] A. Picchi, Q. Wang, F. Ventura, C. Micheletti, J. Heijkoop, F. Picchioni, I. Ciofini, C. Adamo, A. Pucci, Polymers (Basel). 15 (2023). DOI: 10.3390/polym15173530

[24] Q. Zhao, S. Zhang, Y. Liu, J. Mei, S. Chen, P. Lu, A. Qin, Y. Ma, J.Z. Sun, B.Z. Tang, J. Mater. Chem. 22 (2012) 7387. DOI: 10.1039/c2jm16613e

[25] A. Nowak-Król, F. Würthner, Org. Chem. Front. 6 (2019) 1272–1318. DOI: 10.1039/c8qo01368c

[26] O. Krupka, P. Hudhomme, Int. J. Mol. Sci. 24 (2023). DOI: 10.3390/ijms24076308

[27] G. Seybold, G. Wagenblast, Dye. Pigment. 11 (1989) 303–317. DOI: 10.1016/0143-7208(89)85048-X

[28] L. Liu, G. Zhang, J. Xiang, D. Zhang, D. Zhu, Org. Lett. 10 (2008) 4581–4584. DOI: 10.1021/ol801855s

[29] C. Li, J. Yum, S. Moon, A. Herrmann, F. Eickemeyer, N.G. Pschirer, P. Erk, J. Schöneboom, K. Müllen, M. Grätzel, M.K. Nazeeruddin, ChemSusChem 1 (2008) 615–618. DOI: 10.1002/cssc.200800068

[30] X. Lou, Y. Yang, Aggregate 1 (2020) 19–30. DOI: 10.1002/agt2.1

[31] M. Zettl, O. Mayer, E. Klampaftis, B.S. Richards, Energy Technol. 5 (2017) 1037–1044. DOI: 10.1002/ente.201600498

[32] A. Picchi, I. Bettini, M. Ilarioni, M. Carlotti, A. Pucci, RSC Appl. Polym. 2 (2024) 624–633. DOI: 10.1039/D4LP00067F

[33] F.J. Ostos, G. Iasilli, M. Carlotti, A. Pucci, Polymers (Basel). 12 (2020) 2898. DOI: 10.3390/polym12122898

[34] C. Papucci, A. Dessì, C. Coppola, A. Sinicropi, G. Santi, M. Di Donato, M. Taddei, P. Foggi, L. Zani, G. Reginato, A. Pucci, M. Calamante, A. Mordini, Dye. Pigment. 188 (2021) 109207. DOI: 10.1016/j.dyepig.2021.109207

[35] M. Bartolini, C. Micheletti, A. Picchi, C. Coppola, A. Sinicropi, M. Di Donato, P. Foggi, A. Mordini, G. Reginato, A. Pucci, L. Zani, M. Calamante, ACS Appl. Energy Mater. 6 (2023) 4862–4880. DOI: 10.1021/acsaem.3c00362

[36] G. Goti, G. Reginato, C. Coppola, A. Dessì, D. Franchi, A. Mordini, A. Picchi, A. Pucci, A. Sinicropi, L. Zani, M. Calamante, European J. Org. Chem. 27 (2024) 1–10. DOI: 10.1002/ejoc.202400112

[37] C. Papucci, R. Charaf, C. Coppola, A. Sinicropi, M. Di Donato, M. Taddei, P. Foggi, A. Battisti, B. De Jong, L. Zani, A. Mordini, A. Pucci, M. Calamante, G. Reginato, J. Mater. Chem. C 9 (2021) 15608–15621. DOI: 10.1039/d1tc02923a

[38] R. Mori, G. Iasilli, M. Lessi, A.B. Muñoz-García, M. Pavone, F. Bellina, A. Pucci, Polym. Chem. 9 (2018) 1168–1177. DOI: 10.1039/C7PY01933E

[39] A.S. Perera, S. Zhang, S. Homer-Vanniasinkam, M.O. Coppens, M. Edirisinghe, ACS Appl. Mater. Interfaces 10 (2018) 15524–15531. DOI: 10.1021/acsami.8b04774

[40] F. Corsini, A. Nitti, E. Tatsi, G. Mattioli, C. Botta, D. Pasini, G. Griffini, Adv. Opt. Mater. 9 (2021). DOI: 10.1002/adom.202100182

[41] X. Zheng, Q. Peng, L. Zhu, Y. Xie, X. Huang, Z. Shuai, Nanoscale 8 (2016) 15173–15180. DOI: 10.1039/c6nr03599j

[42] F. De Nisi, R. Francischello, A. Battisti, A. Panniello, E. Fanizza, M. Striccoli, X. Gu, N.L.C. Leung, B.Z. Tang, A. Pucci,

Mater. Chem. Front. 1 (2017) 1406–1412. DOI: 10.1039/c7qm00008a

[43] L.R. Wilson, B.C. Rowan, N. Robertson, O. Moudam, A.C. Jones, B.S. Richards, Appl. Opt. 49 (2010) 1651. DOI: 10.1364/AO.49.001651

[44] C. Yang, H.A. Atwater, M.A. Baldo, D. Baran, C.J. Barile, M.C. Barr, M. Bates, M.G. Bawendi, M.R. Bergren, B. Borhan, C.J. Brabec, S. Brovelli, V. Bulović, P. Ceroni, M.G. Debije, J.-M. Delgado-Sanchez, W.-J. Dong, P.M. Duxbury, R.C. Evans, S.R. Forrest, D.R. Gamelin, N.C. Giebink, X. Gong, G. Griffini, F. Guo, C.K. Herrera, A.W.Y. Ho-Baillie, R.J. Holmes, S.-K. Hong, T. Kirchartz, B.G. Levine, H. Li, Y. Li, D. Liu, M.A. Loi, C.K. Luscombe, N.S. Makarov, F. Mateen, R. Mazzaro, H. McDaniel, M.D. McGehee, F. Meinardi, A. Menéndez-Velázquez, J. Min, D.B. Mitzi, M. Moemeni, J.H. Moon, A. Nattestad, M.K. Nazeeruddin, A.F. Nogueira, U.W. Paetzold, D.L. Patrick, A. Pucci, B.P. Rand, E. Reichmanis, B.S. Richards, J. Roncali, F. Rosei, T.W. Schmidt, F. So, C.-C. Tu, A. Vahdani, W.G.J.H.M. van Sark, R. Verduzco, A. Vomiero, W.W.H. Wong, K. Wu, H.-L. Yip, X. Zhang, H. Zhao, R.R. Lunt, Joule 6 (2022) 8–15. DOI: 10.1016/j.joule.2021.12.004

[45] M.G. Debije, R.C. Evans, G. Griffini, Energy Environ. Sci. 14 (2021) 293–301. DOI: 10.1039/D0EE02967J